Available online at www.sciencedirect.com
ScienceDirect
Journal of Organometallic Chemistry 692 (2007) 3121–3132
Journal of Organometallic Chemistry
www.elsevier.com/locate/jorganchem

NO binds to unsaturated Os(IV) polyhydrides as a redox reagent

Joo-Ho Lee, Andrei N. Vedernikov, David Dye, Kenneth G. Caulton *

Department of Chemistry, Indiana University, Bloomington, IN, United States

Received 7 December 2006; received in revised form 30 January 2007; accepted 30 January 2007
Available online 9 February 2007

Abstract

Reaction of $Os(H)_3ClL_2(L{=}P^iPr_3)$ with equimolar NO occurs via a detectable paramagnetic species, to form $OsCl(NO)L_2 + H_2$, then $Os(H)_2Cl(NO)L_2$, together with the product of halogen transfer, $OsHCl_2(NO)L_2$. For comparison, equimolar NO and the dichloride $Os(H)_2Cl_2L_2$ react to give $OsHCl_2(NO)L_2$. DFT(PBE) calculations on potential radical intermediates reveal cases where spin density is on NO (vs. on Os), and show how coordinated H_2 can lead to the observed halogen transfer.

Keywords: Radical; Nitrosyl; Spin densities; Nitroxyl; H atom abstraction; Redox

1. Introduction

NO is a ligand which is highly redox active, including a recently recognized neutral form [1–5]. Even electron species are inherent to the 18-electron rule, as are two electron processes during reaction. The characteristic reactivity patterns of radical complexes are thus underdeveloped. To learn more about transition metal radicals, and especially radicals containing hydride ligands, we have been studying 1:1 (equimolar) reactions which cannot go to an even electron product. For that purpose, the persistent radical NO is one appropriate reactant. An alkyl radical can either abstract a hydrogen atom, to achieve an octet, or it can donate an H atom, to form an unsaturated product. It is of interest to see the extent to which a transition metal hydride can mimic such reactivity patterns.

For clarity, we summarize that a linear NiNO unit is considered as involving 1-electron transfer to the metal, forming NO^+, which then bonds to metal analogous to CO. A bent (~130°) MNO unit is considered NO^-, and sp^2 nitrogen donates a lone pair to bond to 1-electron oxidized metal. The third bonding form involves neutral NO (hence no change in metal oxidation state) and N donates a lone pair to M, while keeping one electron on N (and O); it is a ligand-centered radical.

While chelate complexes can add NO to give a persistent adduct [6], the hydride functionality changes that situation [7,8]. In the reaction of $RuHCl(CO)(P^iPr_3)_2$ with NO (Scheme 1) [9], the NO appears to simply "displace" hydride from half of the metal complex to generate a nitrosyl complex. In addition, a metal hydride is removed from the metal center as HNO. In this way the metal complex avoids having a 17e or 19e configuration, which is rarely persistent [5,10–14].

Scheme 2 shows the mechanism of this reaction, which begins with 1:1 adduct formation, in which spin density resides mainly on the (bent, neutral) NO ligand. The hydride of this initial adduct is removed by a second molecule of NO, so the radical character of NO in the adduct is quenched to yield a diamagnetic compound. The neutral NO ligand is then reduced by Ru to NO^{-1}. The HNO from the quenching of the radical binds to another equivalent of $RuH(CO)Cl(P^iPr_3)_2$ to form the observed nitroxyl complex, $RuH(CO)(HNO)Cl(P^iPr_3)_2$.

At this point we directed our interest to unsaturated polyhydride complexes to establish the impact of having two or more potentially reactive functionalities, the hydrides. In this paper, we discuss the reactions of NO with $Os(H)_3Cl(P^iPr_3)_2$ [15] (**1**) and $Os(H)_2Cl_2(P^iPr_3)_2$ (**2**) [16].

* Corresponding author. Tel.: +1 8128554795; fax: +1 8128553800.
E-mail address: caulton@indiana.edu (K.G. Caulton).

0022-328X/$ - see front matter © 2007 Elsevier B.V. All rights reserved.
doi:10.1016/j.jorganchem.2007.01.059

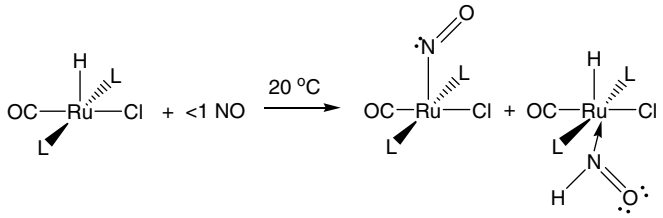

Scheme 1.

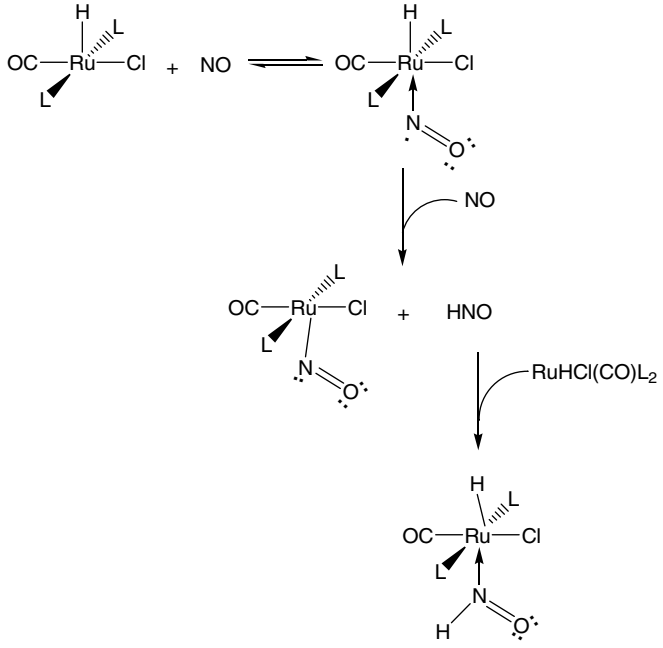

Scheme 2.

2. Results and discussion

2.1. General

The molecules relevant to this study are sketched in Scheme 3, all are diamagnetic and all have been previously characterized [15–20], making their identification here especially rapid. Unsaturated $Os(H)_3ClL_2$ (**1**) is prepared by dehydrohalogenation of $Os(H)_2(H_2)Cl_2L_2$ (**7**) and has a C_{2v} structure. **5** is unusual in having inequivalent hydrides with no evidence of hydride site-exchange fluxionality. Compounds **5** and **6** both have linear nitrosyls, so are saturated. Compound **4** is unsaturated, being linked to **5** by an H_2 oxidative addition equilibrium. Compounds **1** and **2** are both unsaturated and severely distorted from octahedral geometry, and each shows its unsaturation by its ability to form an adduct with H_2 (Eq. (1) and (2)), where the H_2 stays as a diatomic molecular ligand. The *cis* geometry of the two chlorides in **6** is established by the observed diastereotopic inequivalence of the ^{i}Pr methyl ^{1}H NMR signals. Because of an undesirable tendency of free NO to

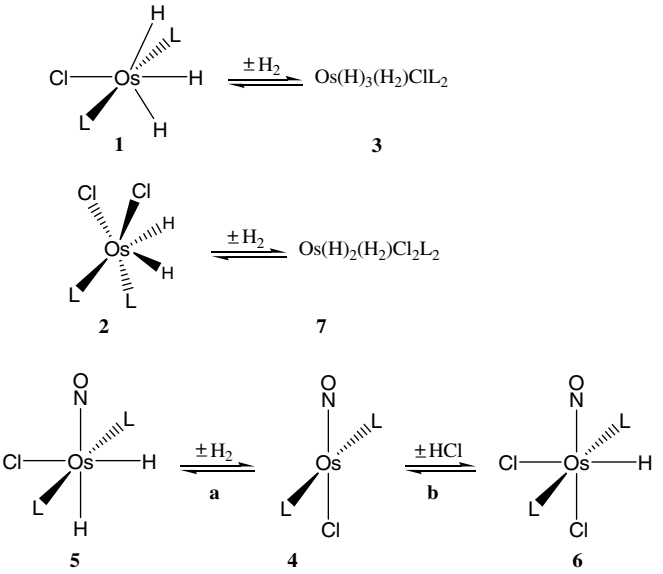

Scheme 3.

convert coordinated NO to coordinated NO_2, we have studied most reactions first with substoichiometric NO, then often evaluated the use of >1 equiv. NO per Os.

2.2. Reaction of $Os(H)_2Cl_2L_2$ with NO

For reasons that will become clear, it is useful to consider first the reaction of NO with $Os(H)_2Cl_2(P^iPr_3)_2$, a 16-electron species with an unusual non-octahedral geometry, due apparently [21] to conflict between steric effects and the geometry preference of electronic configuration d^4.

(a) Reaction products. Reaction of **2** with less than 1 equiv. of NO produced two compounds, $Os(H)_2(H_2)Cl_2L_2$ (**7**) and **6** (Scheme 4), within 3 h. If excess NO is added to **2**, **6** is the only product. Compound **7** is only detected in the reaction of Scheme 4 below 0 °C, consistent with the known weak equilibrium binding of H_2 to **2**.

(b) Low temperature studies. For the investigation of any possible diamagnetic intermediate in the reaction, variable temperature ^{1}H and ^{31}P NMR experiments were carried out with less than 1 equiv. NO per mole of **2**, combined below −78 °C, in toluene. However, no new species was detected from −60 °C to 20 °C. Strong growth of the signal of **6** was detected above 10 °C even though an immediate color change in the reaction mixture from yellow brown to blue was observed at −60 °C. No new species and no **6** were seen until −40 °C, which indicates the blue compound could be a paramagnetic species. The EPR spectrum of a sample which had never been above −90 °C (see 3) shows a rhombic *g* tensor consistent with the structures

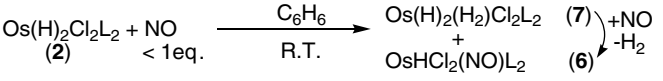

Scheme 4.

calculated by DFT. In addition, the intensity of not only **7** but also **2** increased as the reaction temperature increased due to dissolving of the poorly soluble **2** in toluene. This observation suggests that the NO adduct, $Os(H)_2Cl_2(NO)L_2$ forms at −60 °C, but its further reaction only begins at about 10 °C.

(c) Mechanism. In our DFT(PBE) computational work we have not made a complete survey of the potential energy surface, but rather have focused on the relative energies, the geometric structures and the bonding in the radicals which are candidates to be intermediates in the mechanism. In these computations $^{i}Pr_3P$ ligands (L) were modeled by $Me_3P(L')$. We hope in this way to focus on the features of reactivity which relate specifically to our choice of studying the reaction of a diatomic radical with an unsaturated hydride complex.

*(d) DFT calculations on the reaction of NO with $Os(H)_2Cl_2(PMe_3)_2$ (**2b**).* The overall reaction might be idealized to Eq. (4), where the coefficient 1/2 on product H_2 foretells of mechanistic complexity

$$Os(H)_2Cl_2L_2 + NO \rightarrow OsHCl_2(NO)L_2 + 1/2H_2 \quad (4)$$

and also release of a potential competitive ligand, consumed via Eq. (2). We consider two paths for the reaction of $Os(H)_2Cl_2L_2$ with NO (Scheme 5). These differ by the fate of the 2H following coordination of NO to the reagent complex (which was modelled with $L' = PMe_3$).

Shown in Fig. 1 are two isomers located for the primary adduct; these differ by having the chlorides mutually *cis*(**IIIa**) or *trans*(**IIIb**). Corresponding standard free energies of reaction between **2b** and NO leading to the isomers are given in Fig. 1, indicating that **IIIa** is 7.4 kcal/mol, more stable than **IIIb**. **IIIa** has NO *trans* to chloride (∠Cl(2)–Os–N = 173.25°), and is a "bent nitrosyl." The H(5)–H(30) separation is 1.299 Å and Os–H distances

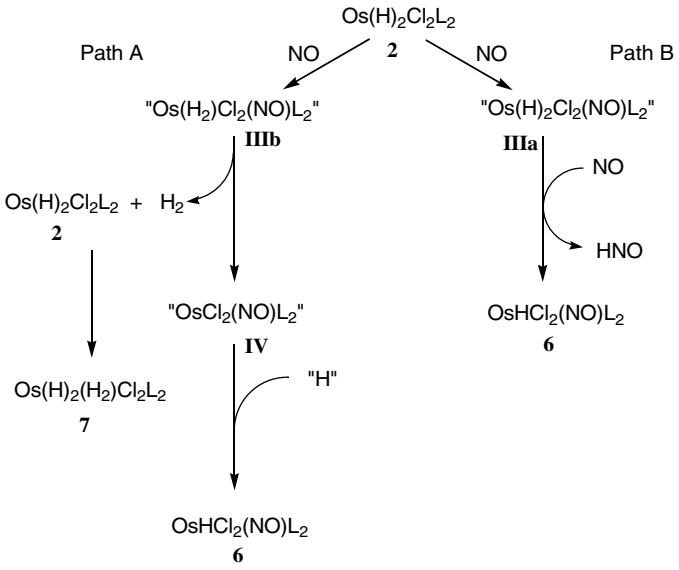

Scheme 5. Complexes in quotation marks were not observed experimentally, but have been studied computationally.

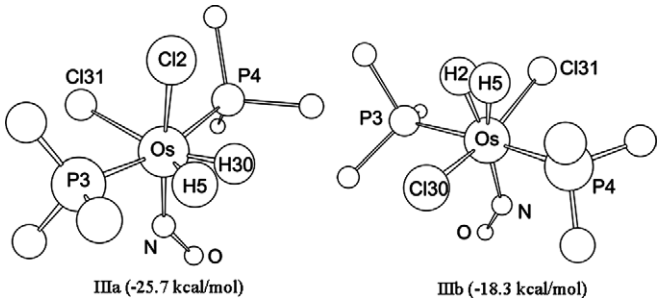

Fig. 1. DFT structures isomer of $Os_2H_2Cl_2(NO)L'_2$.

[22] (1.63 Å to H(30) and 1.64 Å to H(5)) are elongated 0.03 and 0.04, respectively from $Os(H)_2Cl_2(PMe_3)_2$ (Os–H: 1.60 Å). In contrast, the less stable isomer, **IIIb**, has a dihydrogen ligand *trans* to bent NO (∠midpoint [H(2)–H(5)]–Os–N = 179.03 °); the H(2)–H(5) distance, 0.87 Å, clearly indicates a dihydrogen ligand, with increased Os–H distances (Os–H(2) = 1.80, Os–H(5) = 1.83 Å), by nearly 0.2 Å compared to $Os(H)_2Cl_2(PMe_3)_2$. In summary, binding NO *trans* to the hydrides reduces two hydrides to H_2.

In both isomers, the bond angles of ∠Os–N–O (142.62° for **IIIa** and 144.18° for **IIIb**), which are similar to $OsH_3Cl(NO)(PMe_3)_2$ (**Ia**, at 145.53° and **Ib**, at 144.95°, *vide infra*), lie between Os^{+}–$(NO)^{-}$ (∼120°) and Os^{-}–$(NO)^{+}$ (∼180°). In addition, the bond distances of Os–N (1.89 Å for **IIIa** and 1.88 Å for **IIIb**) are relatively longer than those of Os^{+}–$(NO)^{-}$ (=1.86 Å) and Os^{-}–$(NO)^{+}$ (∼1.80 Å). These Os–N distances are very similar to that in compound **Ib** whose NO is *trans* to Cl. Compared to **Ia** (1.97 Å), whose NO is *trans* to hydride (strong *trans* effect), they are shorter. Moreover, the N–O bond distances (1.19 Å for **IIIa** and 1.20 Å for **IIIb**) are between those of $(NO)^{-}$ (1.26 Å) and $(NO)^{+}$ (1.06 Å) and indicate that NO here is a neutral ligand which possesses ligand-centered radical character. It might be expected that **IIIa** has a lower ν_{NO} value than **IIIb** because of the push–pull interaction along Cl(2)–Os–N. However, the DFT calculated vibrational frequencies of both compounds ($\nu_{NO} = 1595\ cm^{-1}$ in **IIIa**, $\nu_{NO} = 1609\ cm^{-1}$ in **IIIb**) are very similar because in **IIIb** NO is *trans* to the weak ligand H_2 and because Os in **IIIb** is reduced by 2e relative to **IIIa**. The resulting strong NO/Os π interaction causes the low vibrational frequency compared to **Ia** ($\nu_{NO} = 1670\ cm^{-1}$) which has the NO ligand *trans* to the hydride. In addition, the NO vibrational motion in **IIIb** is mixed with Os–H(5) vibrational mode. The calculation of spin density supports the conclusion that the NO functions here as a neutral radical. The spin density is mainly localized on the NO ligands (72% for **IIIa** and 82% for **IIIb**), along with a small amount of the density located on other elements (**IIIa**: Os(18%) and Cl(2)(6%), **IIIb**: Os(7%), H(5)(7%) and P(4)(4%)). In the Cl(2) in **IIIa** or H(5) in **IIIb**, spin density could reach these atoms since they interact with the same d orbital with which the NO ligand mixes.

In both compounds, binding NO and increasing the metal coordination number causes slight elongation of bond lengths for Os–Cl (~0.01 Å for **IIIa** and ~0.06 Å for **IIIb**) and Os–P (~0.08 Å for **IIIa** and **IIIb**) compared to $Os(H)_2Cl_2(PMe_3)_2$.

*(e) DFT calculation on candidate intermediate $OsCl_2(NO)(PMe_3)_2$, **IV**.* The energy for releasing H_2 from **IIIa** ($\Delta G^0_{298} = -8.9$ kcal/mol) or **IIIb** ($\Delta G^0_{298} = -16.3$ kcal/mol) indicates that formation of **IV** (Fig. 2) is thermodynamically favorable. In compound **IV**, unpaired electron density is concentrated on the metal center (Os(80%), Cl(4)(5%), Cl(31)(12%)), which indicates one electron oxidation or reduction on the metal center (compared to **III**).

The small amount of spin density on two Cl ligands is explained by mixing of the half-occupied dz^2 and the orbitals of both chlorines. The bond angle Os–N–O (176.8°), vibrational frequency of coordinated NO of 1743 cm^{-1}, and shorter NO bond length (1.19 Å) as compared with that in **IIIa** or **IIIb** all suggest the formation of linear NO ligand (Os^{-}–$(NO)^{+}$). This indicates one electron reduction of the metal center by the NO ligand (to Os(I)). In addition, the relatively shorter Os–Cl(4) distance (2.42 Å) than Os–Cl(31) (2.48 Å) and short bond length of Os–N (1.76 Å) suggest that there is push–pull interaction; the Cl(4) → Os → N angle is 151.6°. From these features, the release of H_2 from the metal center leads to a linear NO ligand, a stronger π-acid than bent NO. In brief, releasing H_2 generates a metal radical (17 electron metal complex, **IV**) by intramolecular electron transfer to Os.

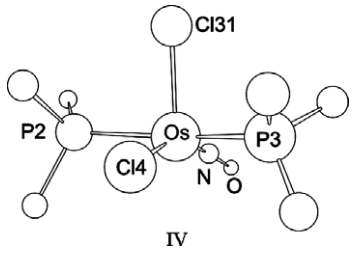

IV

Fig. 2. DFT structure of $OsCl_2(NO)L'_2$.

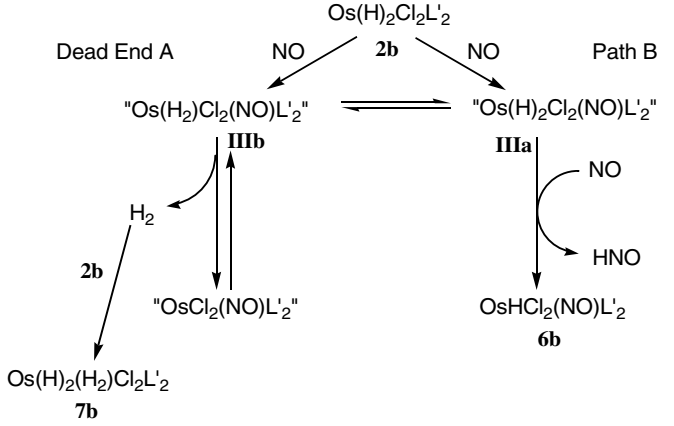

Scheme 6.

(f) Proposed mechanism. The entering NO, in path A, Scheme 6, performs the conversion of hydrides into dihydrogen, which can be transferred to **2b** to produce the H_2 adduct, **7b**. The dehydrogenated complex, $OsCl_2(NO)L'_2$ needs to abstract one H atom from an unknown source to produce **6b**. In contrast, path B shows quenching radical character of **IIIa** by free NO through production of **6b** and HNO, but it cannot explain the observed formation of compound **7**. Therefore (Scheme 6) we propose the operation of dead end path A, but that some of **6b** can result from equilibrium between **IIIa** and **IIIb**, followed by H-atom abstraction from **IIIa** by NO, forming **6b**.

2.3. Reaction of $Os(H)_3ClL_2$ with NO

General. A preliminary general statement is in order. These reactions, even when run at low temperature and with NO limited to ⩽1 mole per mole Os, give a wide range of products, due in part to liberation of H_2 and even HCl from the primary product radical complexes. They are therefore subject to effects of variable mixing rate and the constraints of diffusion control, even though we have tried to achieve effective mixing (all reactions promoted transport of gas to solution by end-over-end tumbling of the NMR tube at a rate of ~20 m^{-1}). Many of the products are apparently derived from kinetically competitive reactions of primary products with released H_2, HCl, and also from available NO (in spite of our keeping the NO:Os ratio at and below 1:1). The reactions are shown to evolve H_2, and H_2 complexes in general are known [23] to be exceptionally strong Bronsted acids, even without any spontaneous elimination of free HCl; this will help to account for a changing number of chloride ligands on a given osmium. Understanding the reactions occurring competitively is clarified somewhat by studies of reactions at various longer times, as well as by some trapping experiments.

(a) Reactions with deficiency of NO. The reaction of $Os(H)_3ClL_2$ ($L = P^iPr_3$) (**1**) with less than one equivalent NO in benzene produced $Os(H)_3(H_2)ClL_2$ (**3**), $Os(H)_2Cl_2L_2$ (**2**), $OsCl(NO)L_2$ (**4**), $Os(H)_2Cl(NO)L_2$ (**5**), and $OsHCl_2(NO)L_2$ (**6**) at 23 °C. Relative yields after 10 min and after 1 day are shown in Scheme 7. Since these reactions did not consume all **1**, the amount of this and its H_2 adduct **3** are not tabulated; **3** is clearly identified by its hydride chemical shift (broad, due to dynamic effects) at about −8 ppm. The deficiency of NO employed in Scheme 7 leaves some **1** unreacted, and its ^1H NMR signal was broad, as was its $^{31}P\{^1H\}$ NMR signal at 54.8 ppm. These features are attributed to Eq. (1). Products were characterized by spectroscopic methods (^1H NMR and $^{31}P\{^1H\}$ NMR) [15,16]. $Os(H)_2Cl_2L_2$ is poorly soluble in aromatic solvents, causing its persistence at short observation times. Over one day of reaction time, free H_2 was observed at 4.48 ppm. $Os(H)_2Cl(NO)L_2$ (**5**) and $OsHCl_2(NO)L_2$ (**6**) can both be seen as secondary products of reaction of $OsCl(NO)L_2$ (**4**) with H_2 and with HCl, respectively (Eq. (3)).

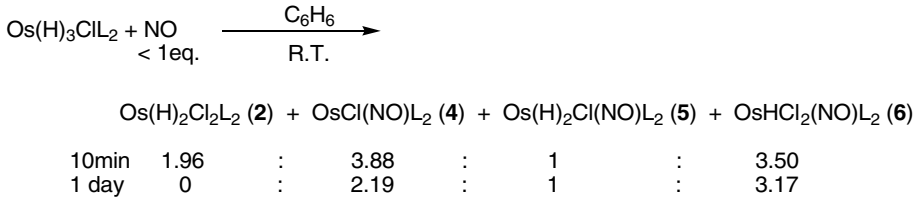

Scheme 7.

(b) Effect of trapping H_2. The growth (Scheme 7) of the ratio R = $Os(H)_2Cl(NO)L_2$ (**5**): $OsCl(NO)L_2$ (**4**) with time suggests that the former results from reaction of the primary product, $OsCl(NO)L_2$, with low levels of free H_2 released from equilibrium 1. The standard state equilibrium position of Eq. (3a) will not necessarily lie far to the left (i.e. oxidized metal) because the strong π-acid NO depletes the reducing power of $OsCl(NO)L_2$. In addition, at nonstandard state concentrations of free H_2, $OsCl(NO)L_2$ is favored. Finally, the rate of achieving the equilibrium at the low H_2 concentrations of our synthetic studies can be variable, and slow.

To test this hypothesis, the reaction of $Os(H)_3ClL_2$ with NO was repeated in the presence of excess $H_2C{=}CHt\text{-}Bu$, intended to scavenge H_2 (and coordinated H) via metal catalysis [24]. Indeed, successful trapping of hydrogen is evident from the observed production of $CEtMe_3$ and the changed ratio *R* of 1:6.8 (vs. 1:1.6 in a comparable experiment omitting $H_2C{=}CHt\text{-}Bu$). In fuller detail, reaction of **1** with NO (<1 equiv.) in the presence of excess *t*-butyl ethylene shows (^1H and ^{31}P NMR evidence), within 10 min, approximately equal amounts of $OsH(Cl)_2(NO)L_2$ and $OsCl(NO)(P^iPr_3)_2$, together with much smaller amounts of $Os(H)_2Cl(NO)L_2$ and $Os(H)_2Cl_2L_2$. The observation of a strong signal for $Os(H)_3Cl(P^iPr_3)_2$ proves that excess NO has been avoided [25]. After 18 h, conversion has changed only negligibly, confirming that rapid uptake of all NO at 10 min observation time.

$OsHCl_2(NO)L_2$ and $OsCl(NO)(P^iPr_3)_2$ and, to a lesser extent, $Os(H)_2Cl(NO)L_2$ and $Os(H)_2Cl_2L_2$ were observed at 10 min and again at 18 h by ^1H and ^{31}P NMR. Between 10 min and 18 h, the main change is a sharpening of both the ^1H and ^{31}P NMR signals of unconsumed $Os(H)_3Cl(P^iPr_3)_2$ as equilibrium 1 responds to decreased $[H_2]$.

(c) Effect of excess NO. To evaluate possible metastability of some of these products, the reaction of excess NO with **1** was also studied. This reaction, observed from 10 m to 24 h, showed complete consumption of **1** and nearly equal amounts of two products, **5** and **6**, together with free H_2. Compound **4** was observed at 10 m, but 60% was gone at 1 h, and absent at 24 h. In spite of excess NO, no dinitrosyl products are produced.

(d) Effect of coordinated H_2. The observed production of **3** above is symptomatic of liberation of H_2. To evaluate directly the effect of additional hydrogen in the reaction system, <1 equiv. NO was added to $Os(H)_3(H_2)ClL_2$ (**3**). This reaction completely consumes **3** within 10 min and forms approximately equal amounts of $OsCl(NO)L_2$, $Os(H)_2Cl(NO)L_2$ and $OsHCl_2(NO)L_2$. This represents an increased yield of $Os(H)_2Cl(NO)L_2$ compared to reaction using $Os(H)_3ClL_2$, and shows more effective trapping of **4** in the presence of additional hydrogen. The product yields were unchanged 4 h later, whereas the reactions in Scheme 7 were still evolving up to 12 h.

(e) Effect of added H_2. The molecules **1**, **2** and **4**, are all competitors to bind any available H_2 and this is the cause of product concentration changes over the timescale of hours. It can be demonstrated that the H_2 adduct of monochloride **1** is more thermodynamically favorable than of dichloride **2**. Addition of excess H_2 to a 1:1 mixture of **1** and **2** shows (NMR) that **1** was completely consumed to form the H_2 adduct, but only approximately 25% of **2** was converted to **7**.

(f) Attempted trapping of HCl. We suggest that the production of a dichloro species from reaction of **1** with NO arises from HCl produced by reductive elimination from some chloride complex. Note (above) that dehydrohalogenation is the synthetic route to **1**. Indeed, in a separate experiment (Scheme 8), the addition of anhydrous HCl to **1** does produce the dichloro-complex, with partial release of H_2.

To confirm the proposed production of HCl from the nitrosyl reaction in Scheme 7, this reaction was repeated in the presence of 10-fold excess NEt_3 as an HCl trapping agent. The experiment indeed showed a diminished amount of dichloride product (based on the integration of hydride signals in ^1H NMR), (Table 1) due to trapping of free HCl by NEt_3, instead of by **1**; this result is true both with a deficiency and an excess of NO.

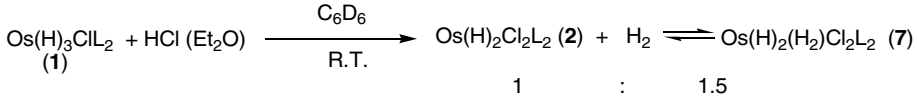

Scheme 8.

Table 1
Effect of added base on the dichloride: mono-chloride ratio 6:5

	Less than 1 equiv. of NO		More than 1 equiv. of NO	
	Without NEt_3	With NEt_3	Without NEt_3	With NEt_3
Ratio of **6/5**	0.6	0.3	0.6	0.2

(g) Low temperature efforts to detect intermediates. To detect possible intermediates, such as an HNO adduct, in the reaction of NO and **1**, NMR experiments were performed by reacting **1** with less than 1 equiv. NO in toluene at low temperature. The proton NMR chemical shift of coordinated HNO is in an unusual and characteristic region (14–22 ppm) and so is highly diagnostic. No new species was observed. At −60 °C, the H_2 adduct of **2**, $Os(H)_2(H_2)Cl_2L_2$ (**7**) appeared and remained until 0 °C [26], then disappeared. Only **2** was observed at room temperature, due to the temperature effect on equilibrium in Eq. (2).

The EPR spectrum of a sample which had never been above −90° (see 3) shows a rhombic *g* tensor and coupling to hydride and one ^{14}N, consistent with the structures calculated by DFT.

*(h) DFT calculation on the formation of $Os(H)_2Cl(NO)(PMe_3)_2$ (**5b**)*. From previously reported work [9] and the experimental evidence from the reactions already discussed, two possible pathways are proposed (Scheme 9). In path A of this scheme, **4b** appears earlier than **5b**, in agreement with experiment; **4b** is produced by H atom abstraction from **IIa** by NO. The standard Gibbs free energy of this H atom transfer reaction is calculated to be +1.7 kcal/mol. HNO is known to be a very short-lived species [27], transforming to N_2O and H_2O. Path B fails to account for production of **4b**. It also fails to produce the observed H_2.

*(i) DFT (PBE) Calculations for formation of NO adduct of $Os(H)_3Cl(PMe_3)_2$, **Ia** and **Ib***. A DFT search for structures for the 1:1 adduct of NO and $Os(H)_3ClL_2$ yielded two minima (Fig. 3) of remarkably similar energy. These differ in the stereochemistry of Cl with respect to NO: *trans* gives **Ib** and *cis* gives **Ia**. Species **Ia** is a trihydride, based on H/H separations of 1.699 Å (H(2)–H(5)) and 1.572 Å (H(5)–H(30)). This also suggests that the oxidation state of the metal center is not changed (Os(IV)). In contrast, **Ib** shows that NO binding *trans* to chloride effects the conversion of two hydride ligands to a dihydrogen ligand whose distance is 0.89 Å (H(5)–H(30)). The cause of this redox conversion also can be understood by the position of three H. Since NO is *trans* to Cl, 2 H are *trans* to one H. The strong *trans* effect of the lone hydride causes weak orbital overlapping (long Os/H distances) between the metal center and the other two H so these two H are converted to one dihydrogen ligand. This contrast to **Ia** indicates a stereoselective conversion, on adding NO, of Os(IV) to Os(II).

In both isomers, the bond angles Os–N–O (145.53° for **Ia** and 144.95° for **Ib**) indicate that NO is not NO^+, since that would be linear. In addition, in both isomers, Os–N bond distances (1.97 Å for **Ia** and 1.88 Å for **Ib**) are relatively longer than Os^-–NO^+ (~1.8 Å) or Os^+–NO^- (=1.86 Å) [28,29]. The N–O distances (1.19 Å for **Ia** and 1.19 Å for **Ib**) lie between those of NO^- (1.26 Å) and NO^+ (1.06 Å) [7] consistent with NO functioning as a neutral, two electron donor; a neutral ligand is expected to possess spin density on the NO ligand, as is found for both **Ia** and **Ib** (90% in **Ia**, 71% in **Ib**). The difference of Os–N distances between **Ia** and **Ib** could be explained by *trans* effect by H(2) in **Ia** or Cl in **Ib**. Hydride has generally high sigma donor ability, lengthening the bond trans to itself. However, Cl is a π-donor (push–pull interaction) to the NO (empty π^* orbital), which gives a shorter Os–N bond length. This push–pull interaction also explains the higher ν_{NO} value in **Ia** ($\nu_{NO} = 1670\ cm^{-1}$) than in **Ib**

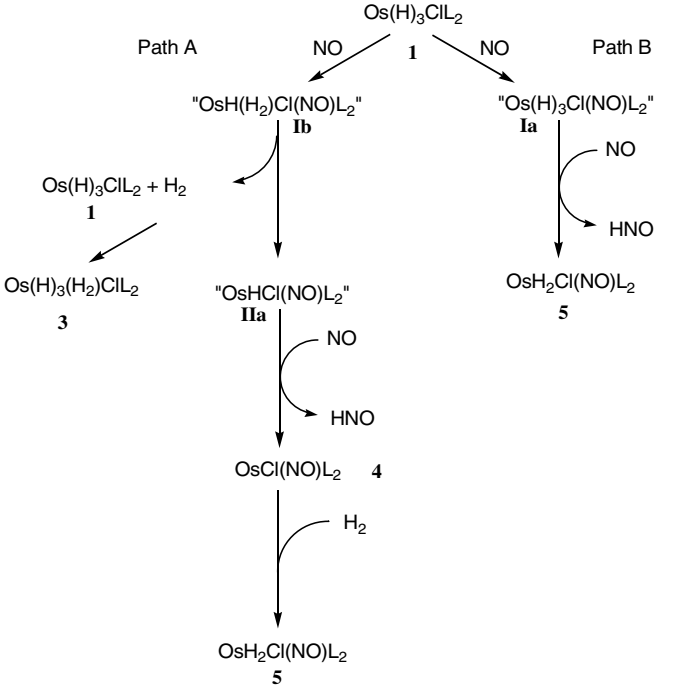

Scheme 9.

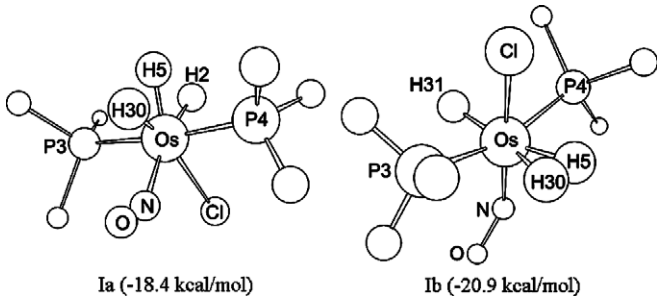

Fig. 3. DFT structures of isomers of $OsH_3Cl(NO)L'_2$.

($\nu_{NO} = 1587\ cm^{-1}$). In spite of these major differences, the energy of these to isomers is remarkably similar.

In addition, the elements which are *trans* to NO also possess unpaired electron density (H(2) in **Ia** = 10%, Cl in **Ib** = 5%), due to interaction between the same d orbital of Os and NO and H(2) or Cl. In the case of **Ib**, a small amount of spin density is located on P(4) (5%) and Os (19%); the differential spin density on only P(4), not also P(3), may due to the direction of the orbital possessing an unpaired electron on NO which is toward P(4). Nevertheless, **Ib** is also correctly described as an NO ligand-centered radical species.

In both isomers, comparing Os–Cl (2.41 Å) and Os–P (2.34 Å) distances in $Os(H)_3Cl(PMe_3)_2$ by DFT geometry optimization, binding NO to the metal center causes elongation of bond lengths for Os–Cl (~0.1 Å for **Ia** and for **Ib**) and Os–P (0.03–0.06 Å for **Ia** and **Ib**), probably due to increasing coordination number.

*(j) DFT calculations for the H_2-loss radical $OsHCl(NO)(PMe_3)_2$, **IIa** and **IIb**.* Releasing H_2 from **Ib** to generate **IIa** (Fig. 4) involves $\Delta G^0_{298} = -7.5$ kcal/mol which indicates that losing H_2 is energetically favorable and due to the stabilizing transoid Cl → Os → NO push/pull interaction in **IIa**. Both isomers resemble distorted square pyramids with axial H(31) for **IIa** (∠N–Os–H = 103.01, ∠Cl–Os–H = 94.50, ∠Cl–Os–N = 162.49) or axial Cl for **IIb** (∠N–Os–Cl = 117.63, ∠H–Os–Cl = 97.20, ∠H–Os–N = 145.18). Isomerization of **IIa** to **IIb** requires $\Delta G^0_{298} = 6.4$ kcal/mol which indicates that placing NO *trans* to Cl, **IIa**, is more favorable than placing NO *trans* to H, **IIb**. This may originate in the better push–pull interaction between Cl–Os–NO in **IIa** as well as the hydride of **IIa** being *trans* to an empty site, a favorable situation. In **IIa**, the spin density is mainly on the metal (Os = 66%, H = 6%, N = 16%, and O = 8%). The Os–N distance (1.78 Å) (shorter than in **Ia** or **Ib**) and the bond angle Os–N–O (171.69°), both consistent with an NO^+ ligand, suggests one electron reduction of the metal center, to Os(I) upon loss of H_2 from **Ia** or **Ib**, as $NO^\circ \rightarrow NO^+ + e^-$. Delocalization of spin density to H also suggests d^7 Os(I), whose unpaired electron is placed in the dz^2 orbital, which interacts with H (Fig. 5). The N–O distance (1.19 Å) in **IIa** is longer than in the NO^+ ion (1.06 Å) [9] due to back donation from the metal center.

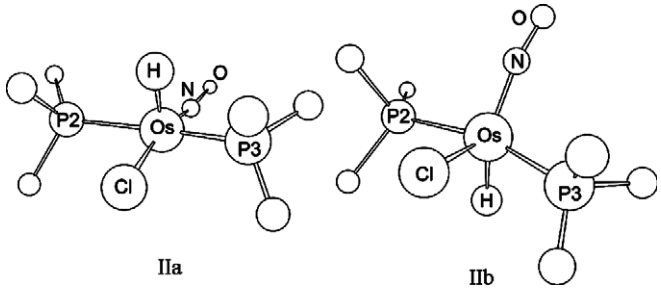

Fig. 4. DFT structure of isomers of $OsHCl(NO)L'_2$.

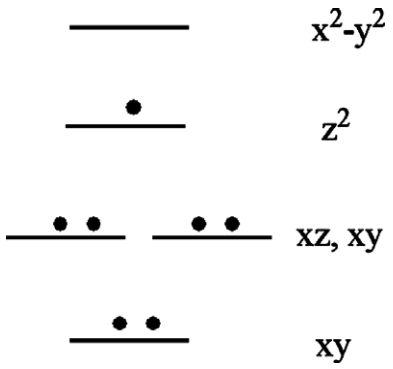

Fig. 5. Electron configuration of square pyramidal d^7 with the *z* axis along Os–H (**IIa**) or Os–Cl (**IIb**).

Deducing oxidation state of DFT structure **IIb** is more difficult than in **IIa**. Spin density in **IIb** is, as in **IIa**, mainly placed on the metal center (Os = 86% and Cl = 15%). The bond length of Os–N 1.78 Å (**IIa**), 1.81 Å (**IIb**) is also shorter than **Ia** (1.97 Å) or **Ib** (1.88 Å). The N–O distance in **IIb** is 1.20 Å. However, the bent character of Os–NO (Os–N–O = 159.4°) is between the neutral NO ligand and the linear NO ligand. In **IIb**, since the strong σ donor hydride is approximately *trans* to NO, thus might weaken back donation to the NO ligand from the metal center and diminish overlap between Os and N which could cause a longer bond distance and more Os–N–O bending than in **IIa**.

The DFT-calculated NO vibrational frequencies of both **IIa** ($\nu_{NO} = 1698\ cm^{-1}$) and of **IIb** ($\nu_{NO} = 1674\ cm^{-1}$) are low. The 1698 cm^{-1} value is quite low for linear NO, due to push–pull interaction of Cl–Os–NO augmented by the low metal oxidation state, Os(I).

In both compounds, releasing H_2 from **Ib** causes no significant change in the bond lengths for Os–Cl (~−0.06 Å for **IIa** and ~−0.02 Å for **IIb**) and Os–P (−0.02 Å ~0.01 Å).

(k) Proposed mechanism. One of the two possible mechanistic pathways in Scheme 9 relies on the known ability of entering CO to convert hydride ligands in **1** to H_2 producing $OsHCl(CO)L_2$ and H_2 [30]; NO, which is known to be a stronger π-acceptor than CO[1], readily performs the same conversion (path A). In contrast, path B requires only a single step from the primary to the final product but it cannot explain the formation and disappearance of **3b** and **4b** observed by NMR monitoring.

(l) Outer- or inner-sphere H-atom transfer. In path B, the best candidate for H atom abstraction from **Ia** to form **5b** is H(2) which has 10% of the spin density. We wanted to establish how unsaturation at Os influenced reactivity towards NO. Saturation of $Os(H)_3ClL_2$ was achieved by forming and characterizing its pyridine adduct, $Os(H)_3ClL_2$(pyridine). This shows no reaction with NO even after 24 h at 22 °C. This shows that NO does not effect outer-sphere H-atom abstraction under our reaction condi-

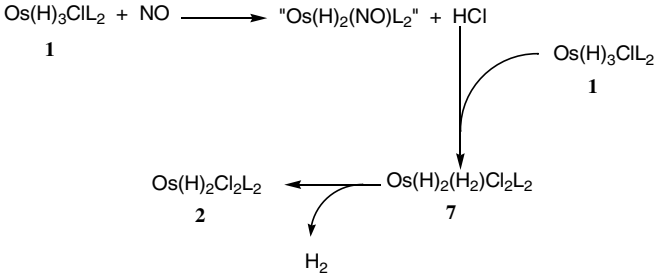

Scheme 10.

tions and that coordination of NO to Os is required for the observed reactions.

*(m) The formation of $Os(H)_2Cl_2L_2$ (**2**) during reaction of $Os(H)_3ClL_2$ (**1**) with NO*. The formation of the dichloro compound from the monochloro compound can be explained by Scheme 10. The entering NO triggers reductive elimination of HCl from the adduct (perhaps preferentially from **Ib**; for example, the ΔG^0 for release of diatomic HCl is only +11.5 kcal/mol, and this can be driven by subsequent reactions of HCl). This HCl can convert the remaining **1** to produce **7** (demonstrated experimentally in Scheme 8).

Why is the chloride transfer operative from OsH_3ClL_2, but not from $OsH_2Cl_2L_2$? The more stable NO adduct of the dichloride is a dihydride (**IIIa**), while the more stable NO adduct of the monochloride is a dihydrogen complex (**Ib**), the latter more Bronsted acidic. Although the energy difference of the less stable redox isomer is not large in either case, perhaps this is the origin of the difference, especially under our low temperature reaction conditions. In any case, the monochloro species behaves as a Bronsted acid (HCl source).

2.4. Summary

In general, the reaction of these Os polyhydrides with the radical NO goes by two pathways which depend on the formation of dihydrogen ligand after coordination of NO. In the primary product, the radical character is mainly located on the nitrosyl N. Due to the π acidic character of NO, two hydrides can form H_2. If an H_2 ligand is formed (**Ib** or **IIIb**), it could be released and trapped by compounds **1**, **2** or **4**. After losing H_2 from **Ib**, the paramagnetic character is located on Os which can be quenched by a second NO to form **4**. If hydrides are not converted to dihydrogen (**Ia** or **IIIa**), the paramagnetic character of the primary products can be diminished through H atom abstraction by the radical NO. Overall in this mechanism, the charge on NO converts from 0 (lone pair donation to metal, **I** and **III**) to +1 (linear NO, three electron donation in **II, IV**, **4**, **5**, and **6**) but has not reached −1 (bent NO, one electron donation). Therefore the overall reaction could be considered two electron reduction of Os which is caused by replacement of H^- by NO^+.

The general features of the chemistry which derives from binding the persistant radical NO to an even electron, unsaturated species are as follows:

(1) Radical products achieve detectable concentrations below −60 °C.
(2) When NO coordinates, it does so as a normal Lewis base (i.e. 2-electron donor), keeping the spin density in one NO π^* orbital, thus leaving spin density on both N and O. Such species are characterized by ∠Os–N–O of 140–150°, which is clearly intermediate between, and distinct from the "fully bent" nitrosyl at 120–130°, or from the linear nitrosyl.
(3) This "half bent" nitrosyl is enough of a π-acid that it can cause the $2H^{-1} \rightarrow H_2 + 2e$ transformation, with 2-electron reduction of the metal, in select cases. Not every odd electron nitrosyl complex has an H_2 ligand, however.
(4) The radical mononitrosyl products of removal of two H, $OsHCl(NO)L_2$ or $OsCl_2(NO)L_2$, generally have spin density predominantly on the metal, with linear NO^+, and thus are best considered as d^7, thus highly reducing (e.g. towards the π-acid nitrosyl ligand).
(5) The 1:1 NO:Os ratios employed here are effective in avoiding production of dinitrosyl complexes, and thus H atom and Cl atom abstractions convert the 5-coordinate species to diamagnetic products.
(6) Because of the reductive eliminations which pervade this chemistry, the resulting decreased metal oxidation states favor linear nitrosyls. These NO^+, derived from NO, further lower the metal oxidation state.
(7) Of interest is why only the NO adduct with $Os(H)_2Cl_2L_2$ has low energy absorption bands (blue color). The more stable NO adduct isomers **Ib** (monochloride) and **IIIa** (dichloride) are oxidation states 2+ (d^6) and 4+ (d^4), respectively. The lower population of d orbitals in the dichloride enables low energy d-to-d transitions. Alternatively, if the transitions are NO → Os charge transfer (forming an NO^+ excited state), this will be easier to Os(4+). An explanation is thus possible regardless of the type of transition and supports the idea that the adducts have different oxidation states and thus only one is a dihydrogen complex.
(8) With regard to the comparison (see 1) to alkyl radical reactivity, both radicals $OsH_3Cl(NO)L_2$ and $OsH_2Cl_2(NO)L_2$ ultimately form saturated species, $OsH_2Cl(NO)L_2$ and $OsHCl_2(NO)L_2$, although not by hydrogen atom abstraction by the radical, as would be the case for an alkyl. Because NO ultimately functions as a 3 electron donor, the radical adduct is in fact a hydrogen atom *donor*. Thus the comparison to alkyl radical reactivity is not fully valid, due to the unusual character of our radical forming moiety, NO. This is because NO can saturate a metal simply by becoming linear MNO (i.e. by 1-electron reduction as $NO \rightarrow NO^+ + e^-$).

3. Experimental

3.1. General consideration

All reactions and manipulations were performed using standard Schlenk line techniques and glovebox under prepurified argon. All solvents were dried and distilled over appropriate agents and stored in airtight solvent bulbs with Teflon closures under argon. All NMR solvents were also dried with appropriate agents and vacuum transferred and stored in a glovebox under the argon. Nitric oxide was used as received. $Os(H)_2Cl_2(P^iPr_3)_2$ [16] was prepared by the reported procedure. $Os(H)_3Cl(P^iPr_3)_2$ was prepared by an improved procedure. All NMR spectra were recorded on Varian Gemini 2000 (300 MHz ^1H, 121 MHz ^{31}P) and Varian Inova (400 MHz ^1H, 161 MHz ^{31}P) spectrometers and referenced by residual protio solvent peaks for ^1H or external standard (phosphoric acid) for ^{31}P. EPR spectra were obtained on a Bruker 300ESP spectrometer operating at X-band (~9.5 GHz): microwave power, 10 mW; modulation amplitude, 5.0 G, modulation frequency, 100 kHz; receiver gain, 8×10^4. All EPR spectra were observed in toluene as frozen glasses at 77 K. The values of unresolved coupling ($A < 5$ G) are derived from the fitting program and are thus less accurate.

Previously unpublished NMR spectra for $OsHCl_2(NO)(P^iPr_3)_2$: $^1H(C_6D_6)$: 2.63(m, CH, ^1Pr), 1.28(5 line pattern due to two overlapping vt); −5.22(t, $J_{PH} = 13.5$ Hz, OsH). $^{31}P\{^1H\}(C_6D_6)$: 14.8(s).

3.2. Improved preparation of $Os(H)_3Cl(P^iPr_3)_2$

0.13 ml of ^{i}PrOH (1.7 μmol) and 0.24 ml of NEt_3 were added to the solution of $Os(H)_2Cl_2(P^iPr_3)_2$ in 30 ml of benzene. After, 2 h stirring, the volatiles were removed by high vacuum with a liquid N_2 trap. 30 ml of pentane was added to the reaction mixture and filtered through 2 cm Celite column to remove $[HNEt_3]Cl$. Pentane was removed by vacuum. 0.43 g of product (91% yield) was collected. The NMR spectra of this product agrees well with reported data [15]. Observing a triplet for the hydride indicates no salt remains. Often the hydride signal appeared as a broad singlet due to some interaction with $[HNEt_3]Cl$.

3.3. Reaction of $Os(H)_3ClL_2$ with a deficiency of NO

Fifteen milligrams of $Os(H)_3Cl(P^iPr_3)_2$ (0.027 μmol) was placed with 0.5 ml of C_6D_6 in an NMR tube equipped with Teflon seal stopcock. This solution was freeze–pump–thaw-degassed three times in liquid N_2 and the headspace evacuated. Eighty millimeters of mercury (mm Hg) of NO (0.011 μmol) was added into the evacuated head space. By melting the frozen solution and shaking, the dark brown solution became yellowish brown. After 10 min at 23 °C, ^1H NMR and $^{31}P\{^1H\}$ NMR spectra showed $Os(H)_2Cl_2(P^iPr_3)_2$, $OsCl(NO)(P^iPr_3)_2$, $Os(H)_2Cl(NO)(P^iPr_3)_2$, and $OsHCl_2(NO)(P^iPr_3)_2$with ratio of 1.96:3.88:1:3.50. Over 2 days, $OsCl(NO)(P^iPr_3)_2$ decreased, but $Os(H)_2Cl(NO)(P^iPr_3)_2$ increased. The ratio of $Os(H)_2Cl_2(P^iPr_3)_2$:$OsCl(NO)(P^iPr_3)_2$:$Os(H)_2Cl(NO)(P^iPr_3)_2$:$OsHCl_2(NO)(P^iPr_3)_2$ was changed to 0:2.19:1:3.17. In addition, presence of $Os(H)_3Cl(P^iPr_3)_2$ confirms the deficiency of NO. The broad singlet hydride for $Os(H)_3ClL_2$ indicates equilibrium with the H_2 adduct, $Os(H)_3(H_2)ClL_2$. ^1H NMR (300 MHz, C_6D_6): −19.43 (bs, $Os(H)_3Cl(P^iPr_3)_2$), −15.82 (t, $J_{PH} = 36$ Hz, $Os(H)_2Cl_2(P^iPr_3)_2$), −10.08 (td, $J_{PH} = 15$ Hz, $J_{HH} = 7.5$ Hz, Os*H*, $Os(H)_2Cl(NO)(P^iPr_3)_2$), −7.6 (bs, $Os(H)_3(H_2)Cl(P^iPr_3)_2$), −5.26 (t, $J_{PH} = 15$ Hz, Os*H*$Cl_2(NO)(P^iPr_3)_2$), −2.22 (td, $J_{PH} = 23.5$ Hz, $J_{HH} = 7.5$ Hz, Os*H*, $Os(H)_2Cl(NO)(P^iPr_3)_2$). $^{31}P\{^1H\}$ NMR (121 MHz, C_6D_6): 14.77 (s, $OsHCl_2(NO)L_2$), 31.63 (s, $Os(H)_2Cl(NO)(P^iPr_3)_2$), 36.97 (s, $OsCl(NO)(P^iPr_3)_2$), 43.5 (s, $Os(H)_2Cl_2(P^iPr_3)_2$), 54.86 (bs, $Os(H)_3Cl(P^iPr_3)_2$).

3.4. Reaction of $Os(H)_3Cl(P^iPr_3)_2$ with excess NO

Fifteen milligrams of $Os(H)_3Cl(P^iPr_3)_2$ (0.027 μmol) was placed with 0.5 ml of C_6D_6 in the NMR tube equipped with Teflon seal stopcock. This solution was freeze–pump–thaw-degassed three times in liquid N_2 and the headspace evacuated. 1 atm of NO was added to the solution. Upon mixing phase, the dark brown solution became pale yellow. After 10 min at 23 °C, ^1H NMR and $^{31}P\{^1H\}$ NMR spectra showed complete consumption of $Os(H)_3Cl(P^iPr_3)_2$ with appearance of compounds 4, 5, and 6 (~1:1.2:1). After 1 day, $OsCl(NO)(P^iPr_3)_2$ had completely disappeared ($^{31}P\{^1H\}$ NMR evidence) and $Os(H)_2Cl(NO)(P^iPr_3)_2$ and $OsHCl_2(NO)(P^iPr_3)_2$ (ratio is 1:0.74) remained.

3.5. Reaction of $Os(H)_2Cl_2(P^iPr_3)_2$ with a deficiency of NO

Ten milligrams of $Os(H)_2Cl_2(P^iPr_3)_2$ (0.017 μmol) was placed with 0.5 ml of C_6D_6 in the NMR tube equipped with Teflon seal stopcock. This solution was freeze–pump–thaw-degassed three times in liquid N_2 and the headspace evacuated. Eighty millimeters of mercury of NO (0.011 μmol) was added to the NMR tube. The brown solution immediately became blue. After 5 min, blue became pale yellow. After 10 min at 23 °C, the ^1H and $^{31}P\{^1H\}$ NMR showed formation of $Os(H)_2(H_2)Cl_2(P^iPr_3)_2$ and $OsHCl_2(NO)(P^iPr_3)_2$. This solution is heterogeneous due to low solubility of $Os(H)_2Cl_2L_2$ in benzene. The reaction was complete in 3 h giving these two products and unreacted $Os(H)_2Cl_2(P^iPr_3)_2$. ^1H NMR (300 MHz, C_6D_6): −10.31 (t, $J_{PH} = 10$ Hz, $Os(H)_2(H_2)Cl_2(P^iPr_3)_2$). $^{31}P\{^1H\}$ NMR (121 MHz, C_6D_6): 23.44 (s, $Os(H)_2(H_2)Cl_2(P^iPr_3)_2$). If 1 atm of NO was applied, only $OsHCl_2(NO)(P^iPr_3)_2$ was present after 3 h.

3.6. Reaction of $Os(H)_3(H_2)Cl(P^iPr_3)_2$ with a deficiency of NO

Ten milligrams of $Os(H)_3Cl(P^iPr_3)_2$ (0.017 μmol) was placed with 0.5 ml of C_6D_6 in an NMR tube equipped with

a Teflon seal stopcock. This solution was freeze–pump–thaw-degassed three times in liquid N_2 and the headspace evacuated. 1 atm of H_2 was added to the NMR tube to produce the H_2 adduct, and the NMR tube was tumbled for 1 h to reach equilibrium. Formation of the H_2 adduct was confirmed by NMR spectrum. The solution of H_2 adduct was frozen and the head space was evacuated. Eighty millimeters of mercury of NO was added to the solution. This reaction was completed in 10 min. Products are described in the text.

3.7. Reaction of $Os(H)_3Cl(P^iPr_3)_2$ with a deficiency of NO in the presence of excess tert-butylethylene

Ten milligrams of $Os(H)_3Cl(P^iPr_3)_2$ (0.018 μmol) was placed with 0.5 ml of C_6D_6 in an NMR tube equipped with a Teflon seal stopcock. 2.3 μL of *tert*-butylethylene was added to the solution. This solution was freeze–pump–thaw-degassed three times in liquid N_2 and the headspace evacuated. Eighty millimeters of mercury of NO (0.011 μmol) was added into the solution. The formation of $OsH(Cl)_2(NO)L_2$ and $OsCl(NO)(P^iPr_3)_2$ and, to a lesser extent, $Os(H)_2Cl(NO)L_2$ and $Os(H)_2Cl_2L_2$ were observed at 10 min and again at 18 h by ^1H and ^{31}P NMR. Between 10 min and 18 h, the main change is a sharpening of both the ^1H and ^{31}P NMR signals of unconsumed $Os(H)_3Cl(P^iPr_3)_2$ (due to the exchange with H_2 in Eq. (1)) as the olefin consumes and thus decreases the available H_2. Hydrogenation of *tert*-butylethylene was observed by ^1H NMR, by the appearance of ethyl and *t*-Bu signals. The ratio of $Os(H)_2Cl(NO)(P^iPr_3)_2$:$OsCl(NO)(P^iPr_3)_2$ is 1:6.8.

3.8. Reaction of $Os(H)_3Cl(P^iPr_3)_2$ with a deficiency (or excess) of NO presence of excess NEt_3

Fifteen milligrams of $Os(H)_3Cl(P^iPr_3)_2$ (0.027 μmol) was placed with 0.5 ml of C_6D_6 in an NMR tube. Thirty-eight microliters of NEt_3 (0.27 μmol) was added to the solution. This solution was freeze–pump–thaw-degassed three times in liquid N_2 and the headspace evacuated. Eighty millimeters of mercury (0.011 μmol) (or 1 atm)of NO was added into the solution. The ratio of $Os(H)_2Cl(NO)(P^iPr_3)_2$:$OsHCl_2(NO)(P^iPr_3)_2$, monitored by NMR over 1 day, was 1:0.3 (1:0.2 with excess NO).

3.9. Reaction of $Os(H)_3Cl(P^iPr_3)_2$ with HCl

Ten milligrams of $Os(H)_3Cl(P^iPr_3)_2$ (0.018 μmol) was placed with 0.5 ml of C_6D_6 in an NMR tube equipped with Teflon stopcock. To this solution, 18.2 μL of HCl (0.018 μmol, 1 M in Et_2O) was added. The dark brown color turned pale yellow in 30 min. The reaction was complete in 30 min to produce a mixture of $Os(H)_2Cl_2(P^iPr_3)_2$ and $Os(H)_2(H_2)Cl_2(P^iPr_3)_2$ with ratio of 1:1.5. Free H_2 was not observed due to broadening of its signal by the equilibrium between $Os(H)_2Cl_2(P^iPr_3)_2$ and $Os(H)_2(H_2)Cl_2(P^iPr_3)_2$.

3.10. Competition reaction between $Os(H)_3Cl(P^iPr_3)_2$ and $Os(H)_2Cl_2(P^iPr_3)_2$ for H_2

Ten milligrams of $Os(H)_3Cl(P^iPr_3)_2$ (0.018 μmol) and 10 mg of $Os(H)_2Cl_2(P^iPr_3)_2$ (0.017 μmol) were placed with 0.5 ml of C_6D_6 in the NMR tube equipped with Teflon seal stopcock. This solution was freeze–pump–thaw-degassed three times in liquid N_2 and the headspace evacuated. Two hundred millimeters of mercury of H_2 (1.9 μmol) was added to the NMR tube. The reaction came to equilibrium in less than 1 h. $Os(H)_3(H_2)Cl(P^iPr_3)_2$, $Os(H)_2Cl_2(P^iPr_3)_2$, and $Os(H)_2(H_2)Cl_2(P^iPr_3)_2$ were observed in the mixture in a ratio of 1:0.75:0.25.

3.11. Attempted reaction of $Os(H)_3Cl(P^iPr_3)_2$(pyridine) with NO

$Os(H)_3Cl(P^iPr_3)_2$(pyridine) was prepared by adding 1.5 μL of pyridine (0.017 μmol) into 10 mg of $Os(H)_3Cl(P^iPr_3)_2$ (0.017 μmol) with 0.5 ml of C_6D_6 in an NMR tube equipped with Teflon seal stopcock. Reaction with pyridine was complete in 10 min with complete consumption of $Os(H)_3Cl(P'Pr_3)_2$ and no evolution of H_2. The reaction mixture was then freeze–pump–thaw-degassed three times using liquid N_2 and the headspace evacuated. Eighty millimeters of mercury of NO (0.011 μmol) was added into the solution. The ^1H and $^{31}P\{^1H\}$ NMR spectra of this solution were unchanged from that of the pyridine adduct after 24 h at 22 °C.

$Os(H)_3Cl(P^iPr_3)_2$(pyridine). ^1H NMR (300 MHz, C_6D_6): −12.76 (t, $J_{PH} = 12$ Hz, 3H, Os*H*), 1.071 (m, 18H, $P(CHMe_2)_3$), 1.26 (m, 18H, $P(CHMe_2)_3$), 2.11 (m, 6H, $P(CHMe_2)_3$), 6.2–10.4 (m, 5H, Os(*pyridine*)). $^{31}P\{^1H\}$ NMR (121 MHz, C_6D_6): 23.44 (s).

EPR studies. We have recorded the EPR spectrum of the blue solution from equimolar $Os(H)_2Cl_2L_2$ and NO in toluene at 77 K; the spectrum (Fig. 6) is reproducible for different prepared samples, and shows structure consistent with a rhombic *g* tensor, with additional structure from ligand hyperfine coupling. Our best fit of the spectrum shows coupling to one ^{14}N and to hydrides, with coupling to P below the spectral resolution, as was true [9] of the previous N-centered radical, $RuHCl(NO)(CO)L_2$. This coupling pattern results from the spin density being heavily located on the nitrosyl. These results support the formation of a 1:1 adduct, and with three different *g* values, in accord with the DFT structures.

We have also recorded the EPR spectrum of the pale yellow solution from equimolar $Os(H)_3ClL_2$ and NO in toluene at 77 K; the spectrum (Fig. 7) shows structure consistent with a rhombic *g* tensor, with additional structure from ligand hyperfine coupling. The spectrum from the fully metal deuterated analog, $Os(D)_3ClL_2$ shows some simplifications, confirming hyperfine coupling to hydrides, but, due to overlap of lines, we were unsuccessful in fitting the spectra to a set of parameters. However, these results again support the formation of a 1:1 adduct,

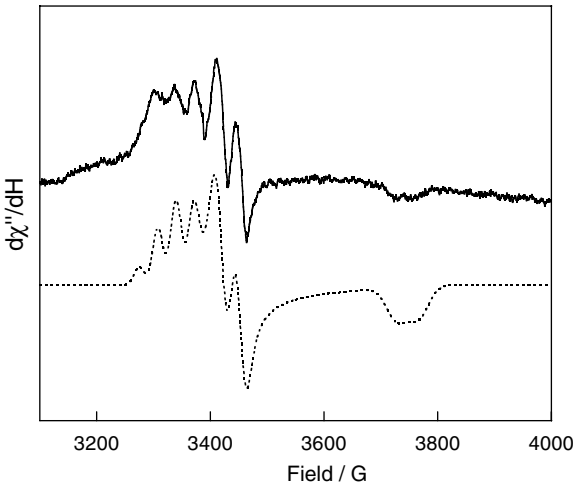

g_x = 2.105	A_x^{H1} = 32.1 G	A_x^{H2} = 39.3 G	A_x^{N} = 35.7 G
g_y = 2.045	A_y^{H1} = 3.7 G	A_y^{H2} = 35.7 G	A_y^{N} = 3.6 G
g_z = 1.877	A_z^{H1} = 3.4 G	A_z^{H2} = 36.2 G	A_z^{N} = 3.9 G

Fig. 6. Observed (solid line) and simulated EPR Spectra of $Os(H)_2Cl_2(NO)(P^iPr_3)_2$.

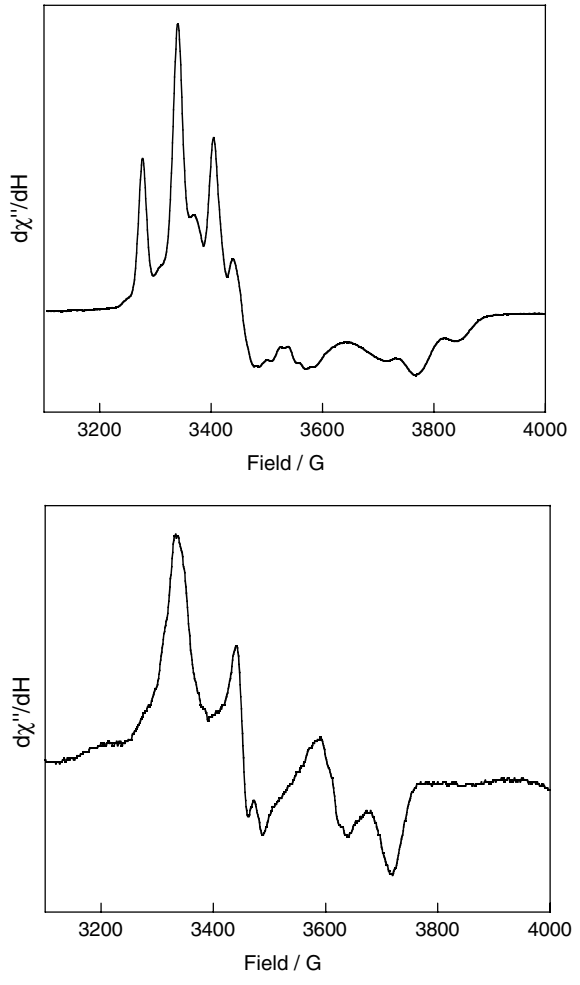

Fig. 7. EPR spectra of $OsG_3Cl(NO)(P^iPr_3)_2$ at 77 K; upper, G = H, lower, G = D.

and with three different g values, consistent with the DFT structures.

Comparison of the two spectra shows that there is none of the other radical in a given sample; each is unique.

3.12. Computational details

Theoretical calculations in this work have been performed using density functional theory (DFT) method [31]; specifically the generalized gradient approximation (GGA) for the exchange-correlation functional by Perdew, Burke and Ernzerhof (PBE) [32] was employed implemented in an original program package "Priroda" [33,34]. In PBE calculations relativistic Stevens–Basch–Krauss (SBK) effective core potentials (ECP) [35–37] optimized for DFT-calculations have been used. Basis set was 311-split for main group elements with one additional polarization p-function for hydrogen, with additional two polarization d-functions for elements of higher periods. Full geometry optimization has been performed without constraints on symmetry using analytical gradients and followed by analytical calculation of the second derivatives of energy with respect to coordinate in order to characterize the nature of the resulting stationary points (minima or saddle points) found on the potential energy surface. For all species under investigation frequency analysis has been carried out. All minima have been checked for the absence of imaginary frequencies. Zero-point vibrational energies and thermodynamic functions were calculated in the harmonic approximation.

Acknowledgement

This work was supported by the National Science Foundation.

References

[1] M. Wolak, R. van Eldik, Coord. Chem. Rev. 230 (2002) 263.
[2] S. Frantz, B. Sarkar, M. Sieger, W. Kaim, F. Roncaroli, J.A. Olabe, S. Zalis, Eur. J. Inorg. Chem. (2004) 2902.
[3] A.V. Marchenko, A.N. Vedernikov, F. Dye David, M. Pink, J.M. Zaleski, G. Caulton Kenneth, Inorg. Chem. 43 (2004) 351.
[4] D.A. Braden, D.R. Tyler, Organometallics 19 (2000) 3762.
[5] D.A. Braden, D.R. Tyler, J. Am. Chem. Soc. 120 (1998) 942.
[6] W.R. Scheidt, M.K. Ellison, Acc. Chem. Res. 32 (1999) 350.
[7] G.B. Richter-Addo, P. Legzdins, Metal Nitrosyls, Oxford University Press, New York, 1992.
[8] T.W. Hayton, P. Legzdins, W.B. Sharp, Chem. Rev. 102 (2002) 935.
[9] A.V. Marchenko, A.N. Vedernikov, D.F. Dye, M. Pink, J.M. Zaleski, K.G. Caulton, Inorg. Chem. 41 (2002) 4087.
[10] D.R. Tyler, Prog. Inorg. Chem. 36 (1988) 125.
[11] D.R. Tyler, F. Mao, Coord. Chem. Rev. 97 (1990) 119.
[12] D.R. Tyler, Acc. Chem. Res. 24 (1991) 325.
[13] D.M. Schut, K.J. Keana, D.R. Tyler, P.H. Rieger, J. Am. Chem. Soc. 117 (1995) 8939.
[14] D.A. Braden, D.R. Tyler, Organometallics 17 (1998) 4060.
[15] D.G. Gusev, R. Kuhlman, G. Sini, O. Eisenstein, K.G. Caulton, J. Am. Chem. Soc. 116 (1994) 2685.
[16] M. Aracama, M.A. Esteruelas, F.J. Lahoz, J.A. Lopez, U. Meyer, L.A. Oro, H. Werner, Inorg. Chem. 30 (1991) 288.

[17] H. Werner, A. Michenfelder, M. Schulz, Angew. Chem., Int. Ed. Engl. 30 (1991) 596.
[18] D.V. Yandulov, W.E. Streib, K.G. Caulton, Inorg. Chim. Acta 280 (1998) 125.
[19] D.V. Yandulov, D. Huang, J.C. Huffman, K.G. Caulton, Inorg. Chem. 39 (2000) 1919.
[20] H. Werner, R. Fluegel, B. Windmueller, A. Michenfelder, J. Wolf, Organometallics 14 (1995) 612.
[21] F. Maseras, O. Eisenstein, New J. Chem. 22 (1998) 5.
[22] P.A. Maltby, M. Schlaf, M. Steinbeck, A.J. Lough, R.H. Morris, W.T. Klooster, T.F. Koetzle, R.C. Srivastava, J. Am. Chem. Soc. 118 (1996) 5396.
[23] Gregory J. Kubas, Metal Dihydrogen and σ-Bond Complexes: Structure, Theory and Reactivity, Kluwer Academic, New York, 1945, c2002.
[24] G. Ferrando-Miguel, J.N. Coalter III, H. Gerard, J.C. Huffman, O. Eisenstein, K.G. Caulton, New J. Chem. 26 (2002) 687.
[25] Indeed, the large amount of unconsumed $Os(H)_3Cl(P^iPr_3)_2$ might be symptomatic of a stoichiometry $Os(H)_3Cl(P^iPr_3)_2 + 2NO \rightarrow OsCl(NO)L_2 + HNO + H_2$.
[26] D.G. Gusev, V.F. Kuznetsov, I.L. Eremenko, H. Berke, J. Am. Chem. Soc. 115 (1993) 5831.
[27] P.J. Farmer, F. Sulc, J. Inorg. Biochem. 99 (2005) 166.
[28] G.R.A. Wyllie, W.R. Scheidt, Chem. Rev. 102 (2002) 1067.
[29] G.R. Clark, J.M. Waters, K.R. Whittle, J. Chem. Soc., Dalton Trans. (1975) 463.
[30] A. Andriollo, M.A. Esteruelas, U. Meyer, L.A. Oro, R.A. Sanchez-Delgado, E. Sola, C. Valero, H. Werner, J. Am. Chem. Soc. 111 (1989) 7431.
[31] R.G. Parr, W. Yang, Density-functional Theory of Atoms and Molecules, Oxford University Press, Oxford, 1989.
[32] J.P. Perdew, K. Burke, M. Ernzerhof, Phys. Rev. Lett. 77 (1996) 3865.
[33] D.N. Laikov, Chem. Phys. Lett. 281 (1997) 151.
[34] D.N. Laikov, Y.A. Ustynyuk, Russ. Chem. Bull. 54 (2005) 820.
[35] W.J. Stevens, H. Basch, M. Krauss, J. Chem. Phys. 81 (1984) 6026.
[36] W.J. Stevens, M. Krauss, H. Basch, P.G. Jasien, Can. J. Chem. 70 (1992) 612.
[37] T.R. Cundari, W.J. Stevens, J. Chem. Phys. 98 (1993) 5555.